

Data-Driven Multiple Resonant Filter Design Integrating Notch Filters and Peak Filters in Dual-Stage Actuator Hard Disk Drives

Masahiro Mae

*Department of Electrical Engineering and Information Systems
The University of Tokyo
Tokyo, Japan
mmae@ieee.org*

Abstract—Magnetic-head positioning performance of hard disk drives in data center infrastructures is fundamental to the large storage capacity. The aim of this paper is to develop a feedback controller design method for hard disk drives integrating robust stabilization and disturbance rejection simultaneously. Notch filters for resonant mode stabilization and peak filters for disturbance rejection are designed simultaneously by resonant filters in the same structure. Multiple resonant filters are designed by frequency response data-driven iterative convex optimization for robust stabilization and disturbance rejection at the same time. The disturbance rejection performance improvement with robust stability is validated in a dual-stage actuator hard disk drive benchmark problem.

Index Terms—Positioning Control, Loop Shaping, Frequency Response, Data-Driven Design, Hard Disk Drive

I. INTRODUCTION

Hard Disk Drives (HDD) that are installed in the data center play an important role in big-data society. The HDD is a mass-produced product and these mechatronic systems have variations of system dynamics. For the feedback controller design in mechatronic systems with model variations, the data-driven robust loop-shaping technique [1], [2] is effective in dealing with variations of the model data set.

Track-following performance is fundamental to the storage capacity of HDD. For the investigation of the track-following performance in HDD, a dual-stage actuator HDD benchmark problem [3] is developed. To improve the disturbance rejection performance with robust stability, several feedback control approaches are introduced using the benchmark problem such as loop-shaping using decoupling controller [4], H_2 and H_∞ optimization [5], [6], Nelder-Mead Simplex Search Algorithm [7], Frequency Response Data (FRD) based optimization using sequential linearization [8], [9], Recurrent Neural Network (RNN) based reinforcement learning [10], Support Vector Machine (SVM) based loop-shaping [11], [12], and loop-shaping using unstable resonant modes [13]. In many of the developed approaches, the feedback controllers are designed in addition to the pre-designed feedback controller in the benchmark problem and the pre-designed feedback controller includes notch filters to stabilize the resonant modes with huge gain. The conservative notch filter design with wide and deep

gain decreasing at resonance frequency has a drawback of the phase delay in low frequency and it results in the low bandwidth in tuning other feedback controllers.

Although important contributions have been made in loop-shaping in HDD, the trade-off between robust stability using notch filters and disturbance rejection performance is not taken into account. In this paper, the developed approach balances the trade-off of the robust stability and disturbance rejection performance by the integrated design of notch filters and peak filters using multiple resonant filters.

The main contributions of this paper are as follows.

- Notch filters for resonant mode stabilization and peak filters for disturbance rejection are designed simultaneously by resonant filters in the same structure.
- Multiple resonant filters are designed by frequency response data-driven iterative convex optimization for robust stabilization and disturbance rejection.

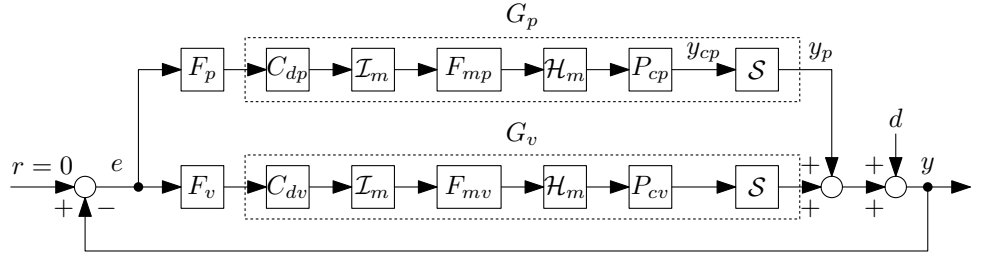
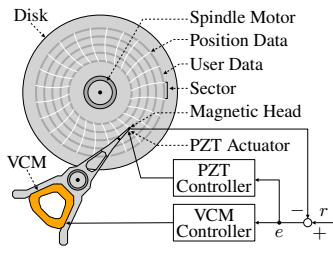
II. PROBLEM FORMULATION

A. Dual-stage actuator hard disk drive

In this paper, the benchmark problem of the magnetic-head positioning control system of a dual-stage actuator HDD [3] is used as the controlled system. It consists of a Voice Coil Motor (VCM) and a piezoelectric (PZT) actuator as shown in Fig. 1(a). The feedback control structure of the dual-stage actuator is shown in Fig. 1(b). The objective of this benchmark problem is to minimize the tracking error $3\sigma(y_c)$ that is evaluated in the worst case of three times of standard deviation value of the continuous-time magnetic head position in steady state response for 1 s against the external disturbance d in Fig. 2. The single-rate sampling frequency is $F_s = 50.4$ kHz. The track pitch is $T_p = 52.7$ nm and the PZT output stroke must be smaller than 50 nm because of stroke limitation.

B. Heuristic multirate notch filter design for gain stabilization

Fig. 3 shows P_c , F_m , and C_d in PZT and VCM. The continuous-time controlled systems P_c have 9 model variations as $k_c = 1, \dots, 9$ drawn in different colors. The discrete-time feedback controller C_d consists of the same one as the example feedback controller in the benchmark problem [3], [4].



(a) Magnetic-head positioning control

(b) Block diagram of dual-stage actuator that consists of continuous-time controlled systems P_c , discrete-time system of a dual-stage actuator HDD feedback controllers C_d , discrete-time multirate filters F_m , interpolator for m times up-sample \mathcal{I}_m , multirate zero-order-hold in m times up-sample \mathcal{H}_m , and sampler \mathcal{S} . The subscripts p and v denote PZT and VCM.

Fig. 1. Magnetic-head positioning control of hard disk drive with dual-stage actuator.

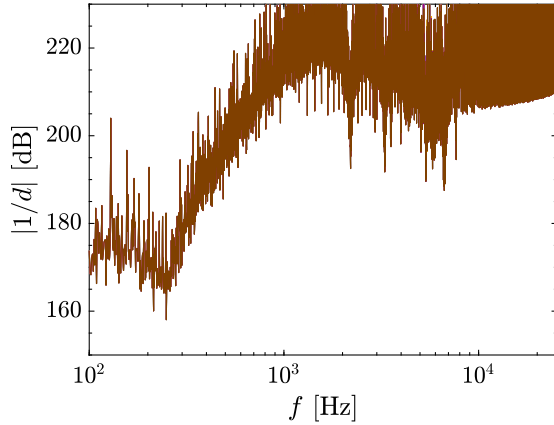


Fig. 2. Inverse disturbance spectrum.

TABLE I
PARAMETERS OF MULTIRATE NOTCH FILTERS.

F_m	ω_m	ζ_n	ζ_d
F_{mp1}	$2\pi \cdot 40000$	0.02	0.5
F_{mp2}	$2\pi \cdot 43000$	0.05	0.3
F_{mv1}	$2\pi \cdot 21000$	0.01	0.15
F_{mv2}	$2\pi \cdot 26000$	0.01	0.15

The multirate notch filters F_m are designed heuristically for gain stabilization of the mechanical resonant modes around and over single-rate Nyquist frequencies. The transfer function of the series-designed multirate notch filter is given by

$$F_m(s) = \frac{s^2 + 2\zeta_n\omega_m s + \omega_m^2}{s^2 + 2\zeta_d\omega_m s + \omega_m^2} \quad (1)$$

where ω_m is the resonance angular frequency. ζ_n and ζ_d are the damping coefficients of numerator and denominator. The parameters of multirate notch filters are shown in TABLE I.

C. Problem description

Fig. 4 shows single-rate systems of G_p and G_v in Fig. 1(b). The controller design problem in this paper is to design F_p and F_v for G_p and G_v integrating notch filters for resonant mode stabilization and peak filters for disturbance rejection at the same time. From the loop-shaping perspective, the sensitivity function of the closed-loop system should follow

the shape of the inverse disturbance spectrum in Fig. 2 with robust stability. The optimization of the feedback controller is addressed by only frequency response data that does not include the parametric model such as fitted transfer functions.

III. DATA-DRIVEN RESONANT FILTER DESIGN INTEGRATING STABILITY AND PERFORMANCE

A. Linearly-structured multiple resonant filters

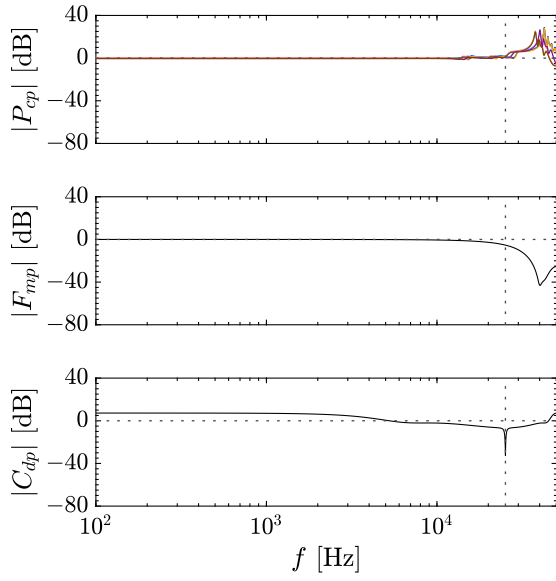
Multiple resonant filters shown in Fig. 5(a) are defined as

$$\begin{aligned} F_{k_u}(j\omega_{k_f}, \rho_{k_u}) &= 1 + \sum_{k_r=1}^{n_r} \frac{\rho_{k_u,(k_r,2)}(j\omega_{k_f})^2 + \rho_{k_u,(k_r,1)}(j\omega_{k_f})}{(j\omega_{k_f})^2 + 2\zeta_{r,k_r}\omega_{r,k_r}(j\omega_{k_f}) + \omega_{r,k_r}^2} \\ &= \begin{bmatrix} 1 \\ \rho_{k_u,(1,1)} \\ \rho_{k_u,(1,2)} \\ \vdots \\ \rho_{k_u,(n_r,1)} \\ \rho_{k_u,(n_r,2)} \end{bmatrix}^T \begin{bmatrix} \frac{1}{(j\omega_{k_f})^2 + 2\zeta_{r,1}\omega_{r,1}(j\omega_{k_f}) + \omega_{r,1}^2} \\ \frac{(j\omega_{k_f})}{(j\omega_{k_f})^2 + 2\zeta_{r,1}\omega_{r,1}(j\omega_{k_f}) + \omega_{r,1}^2} \\ \frac{(j\omega_{k_f})^2}{(j\omega_{k_f})^2 + 2\zeta_{r,1}\omega_{r,1}(j\omega_{k_f}) + \omega_{r,1}^2} \\ \vdots \\ \frac{(j\omega_{k_f})}{(j\omega_{k_f})^2 + 2\zeta_{r,n_r}\omega_{r,n_r}(j\omega_{k_f}) + \omega_{r,n_r}^2} \\ \frac{(j\omega_{k_f})^2}{(j\omega_{k_f})^2 + 2\zeta_{r,n_r}\omega_{r,n_r}(j\omega_{k_f}) + \omega_{r,n_r}^2} \end{bmatrix} \\ &= \rho_{k_u}^T \phi(j\omega_{k_f}) \end{aligned} \quad (2)$$

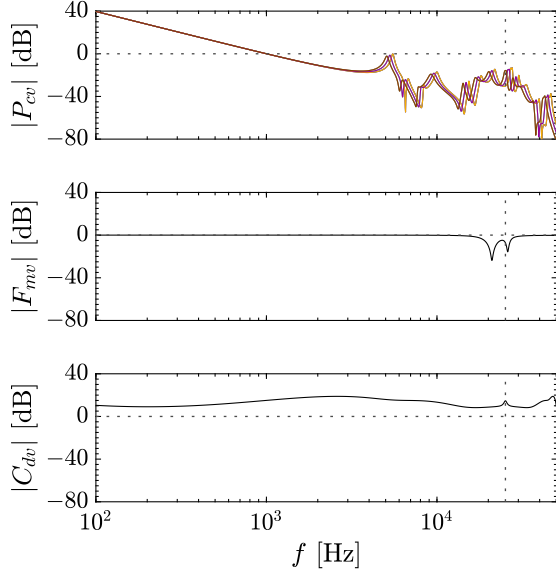
where $k_f = 1, \dots, n_f$ is the index of frequency response data and $k_u \in \{p, v\}$ corresponds each actuator. The number of designed resonance frequency is $n_r \in \mathbb{N}$ and its index is $k_r = 1, \dots, n_r$. The tuning parameter is $\rho = [\rho_p, \rho_v]$ that consists of $\rho_{k_u} \in \mathbb{R}^{2n_r+1}$ with $2n_r$ parameters for each. The resonance angular frequency and the damping coefficient are ω_{r,k_r} and ζ_{r,k_r} . Fig. 5(b) shows the vector locus using a resonant filter and the coefficients ρ_1 and ρ_2 represent the phase and gain of each resonant mode. The resonant filter has the advantage that it can become a notch filter for resonant mode stabilization and a peak filter for disturbance rejection in the same structure by tuning the gain and the phase of the resonant mode.

B. Iterative convex optimization of multiple resonant filters

To minimize the error spectrum with the constraints of PZT stroke limitation, gain stability, and phase stability condition



(a) P_{cp} , F_{mp} , and C_{dp} in PZT.



(b) P_{cv} , F_{mv} , and C_{dv} in VCM.

Fig. 3. Bode magnitude plot of P_c , F_m , and C_d . Vertical black dotted line (.....) denotes Nyquist frequency of single-rate system.

[9], the optimization problem to design multiple resonant filters is given by

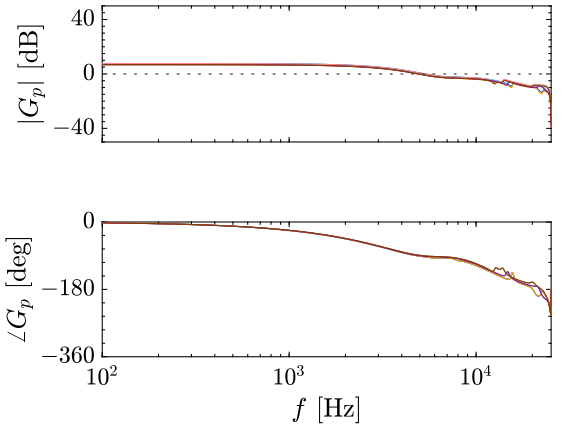
$$\underset{\boldsymbol{\rho}}{\text{minimize}} \quad \max_{\forall k_c, \forall k_f} |e_{k_c}(j\omega_{k_f})| \quad (3a)$$

$$\text{subject to} \quad |y_{p,k_c}(j\omega_{k_f})| \leq y_{p,\max} \quad (3b)$$

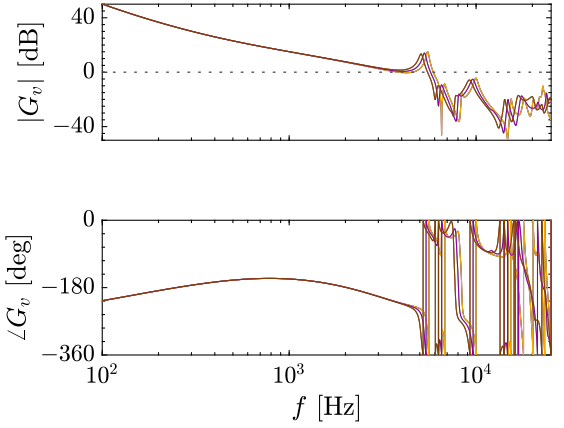
$$w_s(j\omega_{k_f}) |S_{k_c}(j\omega_{k_f}, \boldsymbol{\rho})| \leq 1 \quad (3c)$$

$$|\angle(1 + L_{k_c}(j\omega_{k_f}, \boldsymbol{\rho})) - \angle(1 + L_{0k_c}(j\omega_{k_f}))| \leq \frac{\pi}{2} \quad (3d)$$

where w_s is the weighting of the sensitivity function. The sensitivity function is $S_{k_c}(j\omega_{k_f}, \boldsymbol{\rho}) = (1 + L_{k_c}(j\omega_{k_f}, \boldsymbol{\rho}))^{-1}$



(a) G_p in PZT.



(b) G_v in VCM.

Fig. 4. Frequency responses data of open-loop system.

and the open-loop systems L are defined as

$$L_{k_c}(j\omega_{k_f}, \boldsymbol{\rho}) = L_{p,k_c}(j\omega_{k_f}, \boldsymbol{\rho}_p) + L_{v,k_c}(j\omega_{k_f}, \boldsymbol{\rho}_v) \quad (4)$$

$$L_{p,k_c}(j\omega_{k_f}, \boldsymbol{\rho}_p) = G_{p,k_c}(j\omega_{k_f}) F_p(j\omega_{k_f}, \boldsymbol{\rho}_p) \quad (5)$$

$$L_{v,k_c}(j\omega_{k_f}, \boldsymbol{\rho}_v) = G_{v,k_c}(j\omega_{k_f}) F_v(j\omega_{k_f}, \boldsymbol{\rho}_v) \quad (6)$$

where L_0 is the open-loop system in the initial condition. The error spectrum, the PZT output spectrum and its maximum value are given as follows.

$$e_{k_c}(j\omega_{k_f}) = S_{k_c}(j\omega_{k_f}, \boldsymbol{\rho}) d_{k_c}(j\omega_{k_f}) \quad (7)$$

$$|y_{p,k_c}(j\omega_{k_f})| = \left| \frac{L_{p,k_c}(j\omega_{k_f}, \boldsymbol{\rho}_p) d_{k_c}(j\omega_{k_f})}{1 + L_{k_c}(j\omega_{k_f}, \boldsymbol{\rho})} \right| \quad (8)$$

$$y_{p,\max} = \max_{\forall k_c, \forall k_f} \left| \frac{L_{0p,k_c}(j\omega_{k_f}) d_{k_c}(j\omega_{k_f})}{1 + L_{0k_c}(j\omega_{k_f})} \right| \quad (9)$$

The optimization problem (3) can be solved by iterative convex optimization using sequential linearization [9].

IV. VALIDATION IN DUAL-STAGE ACTUATOR HDD

A. Optimization conditions

The frequency response data includes from 100 Hz to signle-rate Nyquist frequency $F_s/2 = 25.2$ kHz with $n_f = 25101$

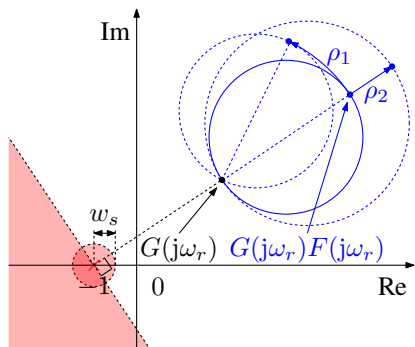
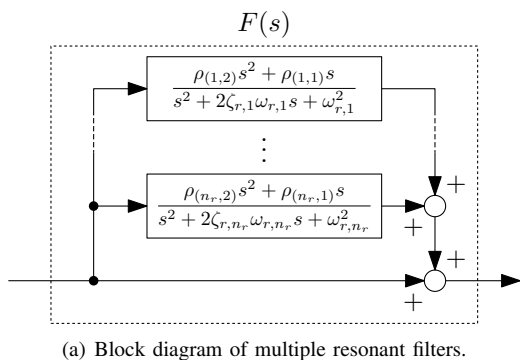


Fig. 5. Multiple resonant filter design.

TABLE II
PARAMETERS OF RESONANT FILTERS BEFORE OPTIMIZATION.

F	ω_r	ζ_r	ρ_1	ρ_2
F_p	$2\pi \cdot 21000$	0.4	-4.2×10^4	7.0×10^{-2}
F_v	$2\pi \cdot 5650$	0.2	-1.4×10^4	5.8×10^{-2}

data points that is the linearly even interval in every 1 Hz. Red lines in Fig. 6 show the multiple resonant filters before optimization that consists of heuristically designed one resonant filter as a notch filter for PZT as shown in Fig. 6(a) and one for VCM as shown in Fig. 6(b), whose parameters are in TABLE II. The controller design and performance before optimization are shown in Fig. 7. The additional seven resonant filters are designed at the frequencies with vertical black dotted lines in Fig. 6, and the damping coefficients of the additional resonant filters are $\zeta_r = 0.02$ with the initial condition of the tuning parameters as $\rho = 0$. The modulus margin of the sensitivity peak is $1/w_s = 6$ dB.

B. Optimization results of multiple resonant filters

The optimization of the eight resonant filters in total is conducted by MATLAB using YALMIP and MOSEK until the improvement of the objective function from the previous iteration becomes less than 0.1%. Blue lines in Fig. 6 show the eight resonant filters in total after optimization. The controller design and performance after optimization are shown in Fig. 8. The optimization results show the loop-shaping of the sensitivity function that follows the shape of the inverse

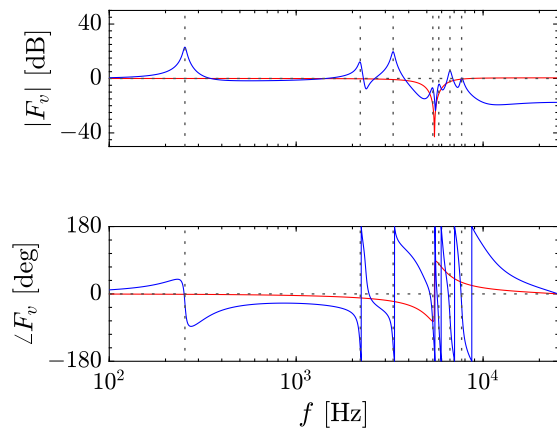
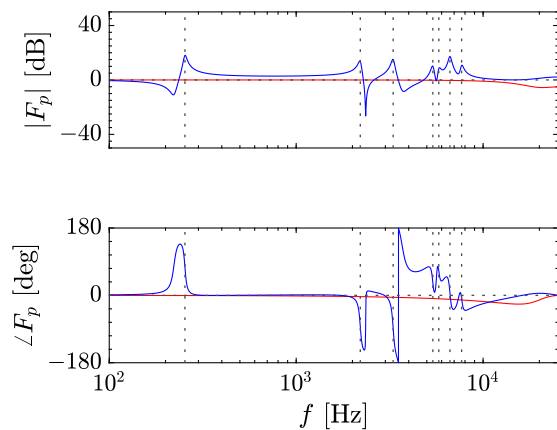


Fig. 6. Frequency responses of resonant filters. Red lines (—) and blue lines (—) are frequency responses before and after optimization, respectively.

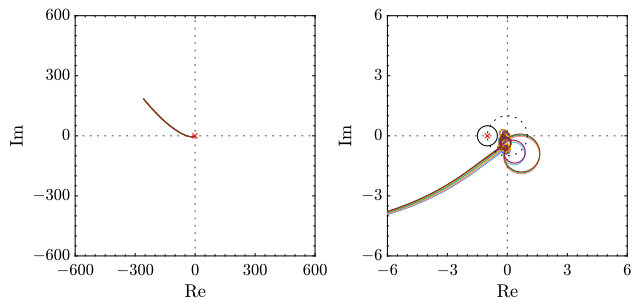
disturbance spectrum with robust stability and a PZT stroke constraint.

C. Performance validation in HDD benchmark problem

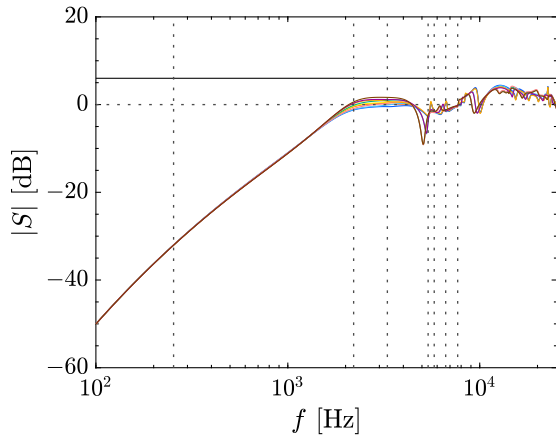
The continuous-time performance validation is conducted in a dual-stage actuator HDD benchmark problem [3]. Fig. 9 shows the track-following performance improvement in time-series error with the optimized resonant filters. Fig. 10 shows that the track-following performance is improved in all 9 cases with satisfying the maximum stroke of a PZT actuator. As a result, the disturbance rejection performance improvement with optimized resonant filters is validated.

V. CONCLUSION

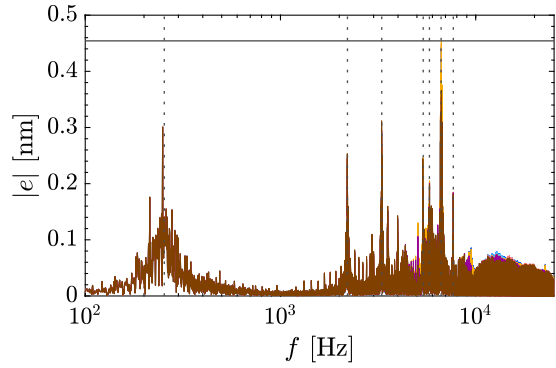
In this paper, the design method of multiple resonant filters integrating notch and peak filters is developed. Notch filters for resonant mode stabilization and peak filters for disturbance rejection are designed simultaneously by resonant filters in the same structure. Multiple resonant filters are designed by frequency response data-driven iterative convex optimization for robust stabilization and disturbance rejection at the same time.



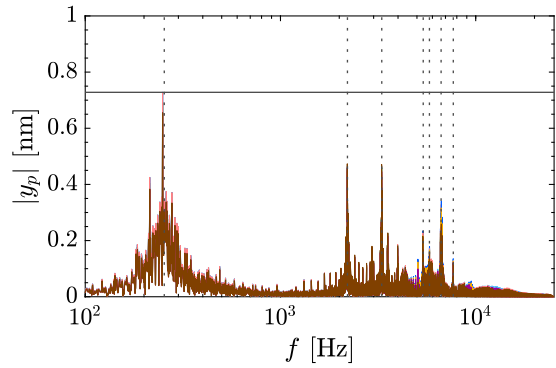
(a) Nyquist diagram.



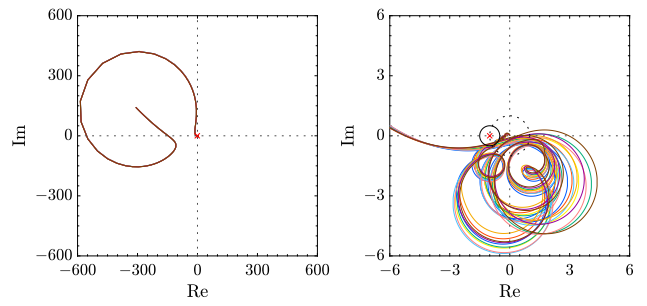
(b) Sensitivity function.



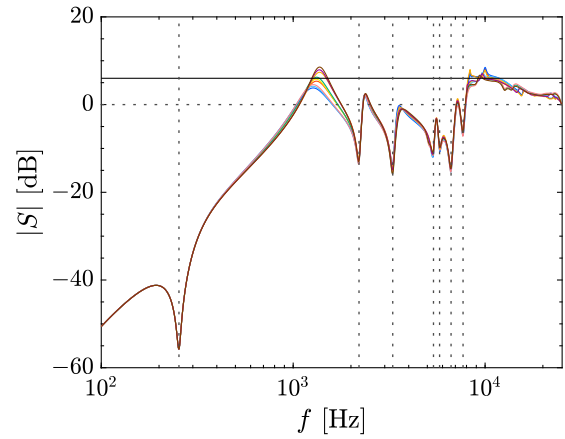
(c) Error spectrum.



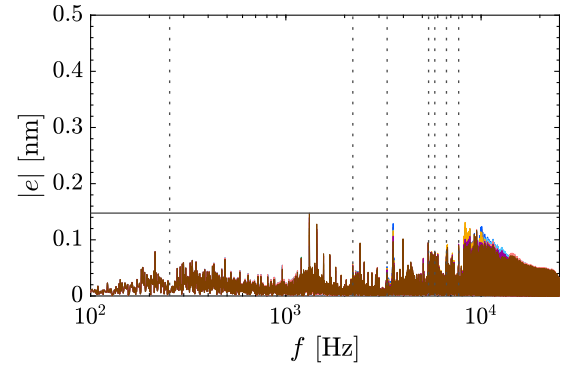
(d) PZT output spectrum.



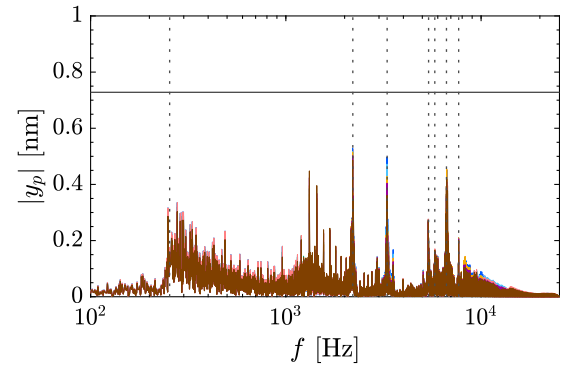
(a) Nyquist diagram.



(b) Sensitivity function.



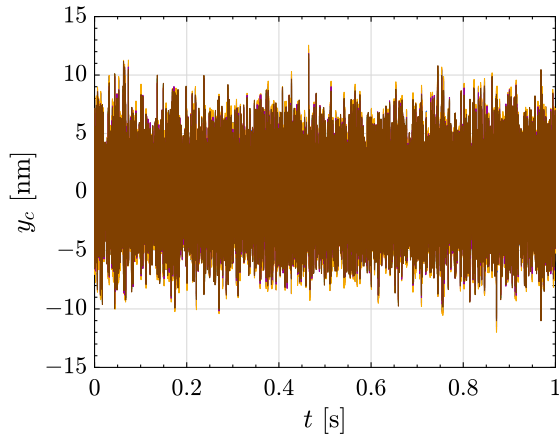
(c) Error spectrum.



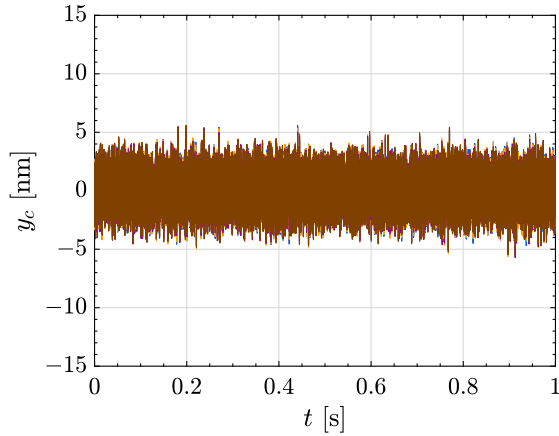
(d) PZT output spectrum.

Fig. 7. Controller design before optimization. Vertical black dotted lines (----) correspond to resonance frequencies of additional seven resonant filters.

Fig. 8. Controller design after optimization. Vertical black dotted lines (----) correspond to resonance frequencies of additional seven resonant filters.



(a) Before optimization.



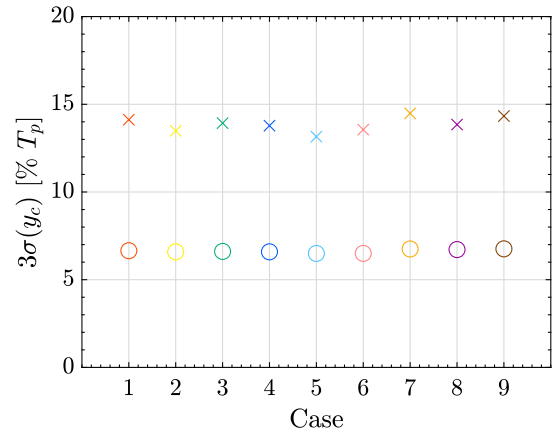
(b) After optimization.

Fig. 9. $y_c(t)$: time-series track-following performance.

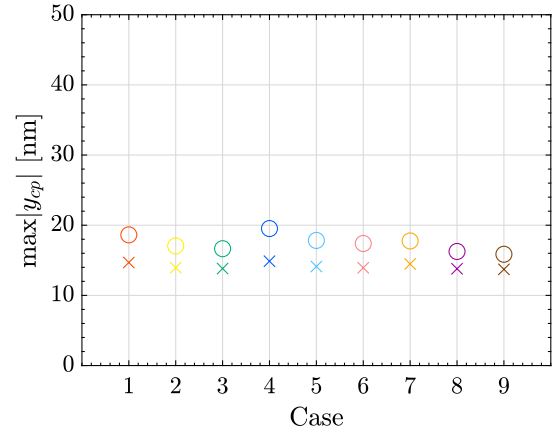
The disturbance rejection performance improvement with robust stability is validated in a dual-stage actuator HDD benchmark problem. Ongoing research focuses on the controller structure and integrated design with multirate filters.

REFERENCES

- [1] T. Shiohara and Y. Maeda, "Enhanced Auto-Tuning of Feedback Controllers with Aggressive Search Ensuring Stability and Its Application to Galvano Scanner," *IEEJ Journal of Industry Applications*, vol. 13, no. 5, pp. 539–546, 2024.
- [2] E. Kuroda, Y. Maeda, and M. Iwasaki, "Efficient Autonomous Design of Cascade Structure Feedback Controller Parameters Realizing Robust Stabilization," *IEEJ Journal of Industry Applications*, vol. 13, no. 1, pp. 34–40, 2024.
- [3] T. Atsumi, "Magnetic-head positioning control system in HDDs," <https://jp.mathworks.com/matlabcentral/fileexchange/111515>, 2022.
- [4] —, "Benchmark Problem for Magnetic-Head Positioning Control System in HDDs," in *The 22nd IFAC World Congress*, vol. 56, 2023, pp. 8790–8796.
- [5] N. Prakash, J. Seo, A. Rose, and R. Horowitz, "Data-driven track following control for Dual Stage-Actuator hard disk drives," in *The 22nd IFAC World Congress*, 2023, pp. 11 380–11 383.
- [6] M. Hirata, J. Shimokasa, and M. Suzuki, "Two-Step Design of H_∞ Controller for Dual Stage Hard Disk Drives," in *The 22nd IFAC World Congress*, 2023, pp. 11 376–11 379.
- [7] S. Bashash, "Application of MIMO data driven feedback control design to dual stage hard disk drives," in *The 22nd IFAC World Congress*, 2023, pp. 11 402–11 405.
- [8] X. Wang, W. Ohnishi, and T. Atsumi, "Systematic Filter Design by Convex Optimization for Disturbance Rejection in Dual-Stage Actuated Hard Disk Drives," in *The 22nd IFAC World Congress*, vol. 56, 2023, pp. 10 608–10 613.
- [9] M. Mae, W. Ohnishi, and H. Fujimoto, "Frequency Response Data-based Resonant Filter Design considering Phase Stabilization and Stroke Limitation applied to Dual-Stage Actuator Hard Disk Drives," in *The 22nd IFAC World Congress*, vol. 56, 2023, pp. 10 614–10 619.
- [10] R. Muto and Y. Uchimura, "Controller design for HDD benchmark problem using RNN-based reinforcement learning," in *The 22nd IFAC World Congress*, vol. 56, 2023, pp. 4424–4429.
- [11] T. Atsumi, S. Yabui, and S. Nakadai, "Optimization Method for Magnetic-Head Positioning Control System in HDD Against Unexpected Plant Perturbations by Using Data Mining Techniques," *IEEE transactions on magnetics*, vol. 60, no. 1, pp. 1–14, 2024.
- [12] H. Murakami and S. Yabui, "Loop Shaping Method Based on Data Considering Mechanism Constraints for Each Actuator in DISO Magnetic Head Position Control System in HDDs," in *2024 IEEE 18th International Conference on Advanced Motion Control (AMC)*. IEEE, 2024, pp. 1–6.
- [13] T. Atsumi, S. Yabui, A. Okuyama, and M. Mae, "Loop-shaping method with unstable poles for magnetic-head positioning control in hard disk drive," in *2024 IEEE International Conference on Advanced Intelligent Mechatronics (AIM)*. IEEE, 2024, pp. 818–823.



(a) $3\sigma(y_c)$: track-following performance.



(b) $\max|y_{cp}|$: PZT output maximum stroke.

Fig. 10. Robust performance before (\times) and after (\circ) optimization.